Journal of Theoretical and Applied Physics (2020) 14:137–147
https://doi.org/10.1007/s40094-020-00370-9

RESEARCH

Effect of Gd^{3+} on optical and thermal properties of tellurite glass

M. N. Azlan[1] · C. Eevon[2] · M. K. Halimah[2] · R. El-Mallawany[3] · S. L. Hii[2]

Received: 12 June 2019 / Accepted: 4 March 2020 / Published online: 17 March 2020

Abstract
The study of optical and thermal properties of gadolinium oxide-doped tellurite glass was studied for the first time to the best of our knowledge. Gadolinium oxide-doped tellurite glass system with chemical formula $(1-x)[(TeO_2)_{70}(B_2O_3)_{30}]$-$x(Gd_2O_3)$ with $x=0.2$, 0.4, 0.6, 0.8 and 1.0 mol% was prepared by the melt-quenching technique. X-ray diffraction spectroscopy, Fourier transform infrared spectroscopy, UV–Vis spectroscopy and EL X-02 high-precision ellipsometer have been carried out. The thermal diffusivity of the amorphous material was studied using laser flash method. The microanalysis of major elements in the glass was examined by employing energy-dispersive X-ray spectrometry. The IR of the glass matrix denotes three obvious absorption bands which are assigned to TeO_4, BO_3 and BO_4 vibrational groups. The addition of Gd ions enhances the refractive index of the tellurite glass. The optical band gap and Urbach energy were determined based on the absorption spectra. It is found that the Gd ions reduce the optical band gap energy. The thermal diffusivity of the glass samples follows nonlinear trend with the concentration of Gd ions. Electronic polarizability, optical basicity and metallization criterion have been calculated for every glass composition. Based on these results, the proposed materials have high potential to be applied in photonic materials.

Keywords Glasses · Tellurite · Rare earth · Optical · Thermal

Introduction

Within the last few decades, research in tellurite glass has raised due to its high capability to be used in various optical applications. Tellurite-based glass containing transition metals or rare earths had been increasingly studied [1–19]. The incorporation of borate oxide in tellurite glasses is the most stable glass and had been widely used due to their attractive characteristics which have potential used for specific applications [3]. In addition, the high stability glass with low melting temperature is highly important to reduce the energy consumption during the fabrication process. Some physical properties of tellurite glasses as smart materials have been reported recently [4]. The inclusion of different oxides in tellurite glass had been studied in various kinds of applications [1–19].

The study of gadolinium oxide-doped tellurite glass on its optical and thermal properties has not been well investigated. There are few progresses in gadolinium-doped tellurite glass in terms of physical, optical and thermal properties. It is found that the gadolinium oxide gives significant effect to the optical properties of tellurite glass as it has sharp spectral lines, high refractive index and high potential to produce laser emission. Hence, in this research, the study of gadolinium-doped tellurite glass is performed to offer the alternative photonic materials other than erbium-doped tellurite glass.

In this contribution, we report the impact of gadolinium oxide on the physical, structural, optical and thermal properties of tellurite glass in the form: $(1-x)[(TeO_2)70(B_2O_3)30]$-$x(Gd_2O_3)$ with $x=0.2$, 0.4, 0.6, 0.8 and 1.0 mol%. The physical, structural, optical and thermal parameters are the density, molar volume, XRD and FTIR analysis, refractive index, optical band gap and thermal diffusivity. Herein, we have underlined a systematic strategy to evaluate the

✉ R. El-Mallawany
raoufelmallawany@yahoo.com

[1] Physics Department, Faculty of Science and Mathematics, Sultan Idris Education University, 35900 Tanjong Malim, Perak, Malaysia

[2] Physics Department, Faculty of Science, University Putra Malaysia (UPM), 43400 Serdang, Selangor, Malaysia

[3] Physics Department, Faculty of Science, Menoufia University, Shibin Al Kawm, Egypt

performance of gadolinium-doped tellurite glass to be used in photonic application.

Experimental

The gadolinium-doped tellurite glass with chemical composition of $(1-x)[(TeO_2)_{70}(B_2O_3)_{30}]$-$x(Gd_2O_3)$ with $x = 0.2$, 0.4, 0.6, 0.8 and 1.0 mol% was successfully fabricated (Table 1). The high-purity oxides for the studied glass system were mixed in an alumina crucible. The mixture was placed in the electric furnace at 400 °C for 1 h to eliminate the water vapour in the mixture. The mixture was then melted in the furnace at 900 °C for 2 h followed by rapid quenching into a cylindrical stainless-steel mould. The mould containing the glass sample was annealed at 350 °C for 1 h to avoid the formation of air bubbles as well as to eliminate thermal strains and enhance the mechanical strength of the sample. The glass sample was allowed to cool down at room temperature for 4 h. The prepared glass samples were cut and polished on the both sides to obtain a parallel and clear surface.

The XRD pattern was obtained by using Phillips X-ray Diffractometer X'Pert Pro PW 304. The microanalysis of major constituents was examined using energy-dispersive X-ray spectrometry (EDX) with an Oxford Inca analyser. The accuracy of this instrument is $(2\theta) < 1.5\%$. FTIR transmittance spectra of the samples were investigated using a Mattson 5000 FTIR Spectrometer (2000–200 cm^{-1}). The error of this instrument is ± 10 µm. The density of the samples was measured using electronic densimeter MD-300S with standard error of ± 0.0001 which is based on Archimedes' principle with distilled water as the buoyant liquid. UV–Vis absorption spectra have been recorded by using Shimadzu-1650PC UV–Vis spectrophotometer (200–1000 nm). In cases where a sample spectrum is measured and the peaks must be specified within an error of 1 nm, a wavelength accuracy of ± 0.1 nm is probably adequate. The refractive index was measured using EL X-02 high-precision ellipsometer (632.80 nm). The standard error of this instrument is ± 0.1 nm. The thermal diffusivity of the glass samples was obtained by photoflash technique using a K-type thermocouple. A normal electronic camera flash (Maxxum, model 5400HS) as an energy pulse source was positioned 2 cm from front surface of the sample. A disc-shaped sample was placed on the sample holder, and the K-type thermocouple was attached to the back surface of the sample. The front block of the sample was covered with the aluminium foil to shield the light from the photoflash reaching any pan of the thermocouple.

In this setup, a fast response K-type thermocouple was attached directly to the rear surface of the sample to monitor the temperature at the rear surface of the sample. The signal from the thermocouple was then amplified by a preamplifier (SR560) and monitored by the digital oscilloscope (Tektronix TDS 220). The signal was then analysed for thermal diffusivity value. The photodiode (model RS 308(067) was used to trigger the oscilloscope. A period of 10 min was allowed in between the measurements in order to make sure the sample has reached the initial temperature (room temperature) before proceeding to a new measurement.

Results and discussion

XRD, EDX and FTIR spectra

It is observed that the XRD pattern of the prepared glasses does not reveal any distinguishable peaks but exhibit broad diffusion hump at low scattering angles ($2\theta = 20$–$40°$) as shown in Fig. 1 and Table 2. Figure 2 represents the EDX spectra obtained for gadolinium oxide tellurite glass samples. It can be seen from Fig. 2 that the glass samples have not shown any contamination by other elements. The FTIR spectra consist of the absorption bands implying the local structural within the vitreous network as shown in Fig. 3. The assignments for each IR bands are based on the previous reported literature and collected in Table 2. The tellurium network is comprised of two vibrational modes [5]:

I. 600–640 cm^{-1} is due to Te–O vibration in trigonal bi-pyramids, TeO_4,
II. 680–700 cm^{-1} corresponds to Te–O vibration in trigonal pyramid, TeO_3.

The absorption bands for borate glass can be divided into three vibrational regions:

I. For 600–800 cm^{-1}, it is bending vibration of various borate arrangements B–O–B [20, 21],
II. For 800–1200 cm^{-1}, it is assigned to stretching vibration of B–O bonds from tetrahedral BO_4 units [20, 21],

Table 1 The chemical composition of $(1-x)[(TeO_2)_{70}(B_2O_3)_{30}]$-$x(Gd_2O_3)$ glass sample

x (mol%)	TeO_2	B_2O_3	Gd_2O_3	Total (%)
0.2	83.7904	15.6647	0.5448	100
0.4	83.3346	15.5795	1.0859	100
0.6	82.8818	15.4949	1.6233	100
0.8	82.4322	15.4108	2.1570	100

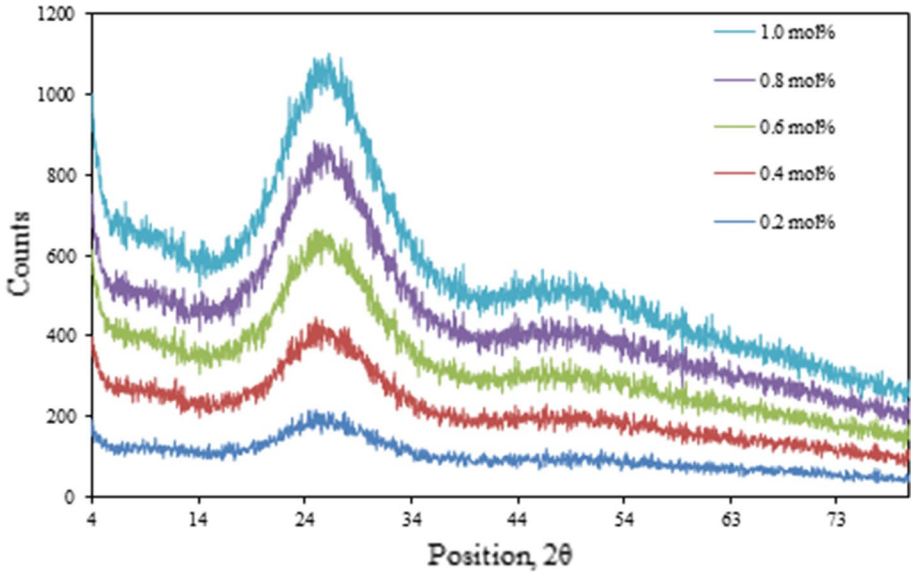

Fig. 1 X-ray diffraction pattern of $(1-x)[(TeO_2)_{70}(B_2O_3)_{30}]$-$x(Gd_2O_3)$ glasses

Table 2 Assignment of IR transmission bands of $(1-x)[(TeO_2)_{70}(B_2O_3)_{30}]$-$x(Gd_2O_3)$ glasses

No.	0.2	0.4	0.6	0.8	1.0	Assignments
1	1369	1350	1370	1357	1370	Trigonal B–O bond stretching vibrations in isolated trigonal BO_3 units [5, 12]
2	1222	1219	1225	1218	1224	Trigonal B–O bond stretching vibrations of BO_3 units from boroxyl groups [5, 12]
3	630	625	645	643	622	TeO_4 groups present in all tellurite-containing glass [5, 12]

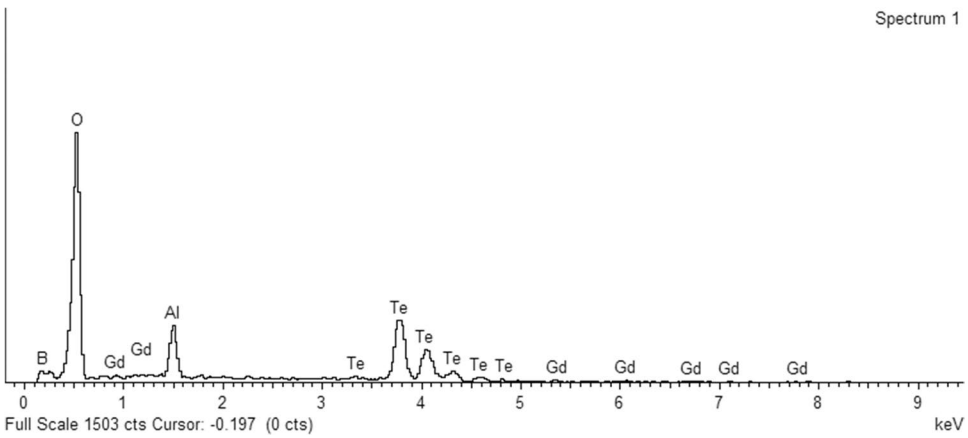

Fig. 2 Energy-dispersive X-ray spectrum of $(1-x)[(TeO_2)_{70}(B_2O_3)_{30}]$-$x(Gd_2O_3)$ glasses ($x=0.8$ mol%)

III. For 1200–1800 cm^{-1}, it is due to the stretching vibration of B–O bonds of trigonal BO_3 units [5].

It can be seen that the FTIR spectra for the presently studied non-crystalline samples are found to be around 621–646 cm^{-1}, 1217–1225 cm^{-1} and 1349–1371 cm^{-1}. The absorption band around 621–646 cm^{-1} is attributed to the Te–O–Te bridges between tellurium atoms [TeO_4]. The peaks at 1217–1225 cm^{-1} are allotted to the trigonal B–O bond stretching vibrations of BO_3 units. Band at 1349–1371 cm^{-1} implies the B–O stretching vibration of BO_3 units.

Density and molar volume

Density and molar volume of gadolinium oxide-doped tellurite glasses are presented in Table 3 and Fig. 4. The increase in density 3914 to 4101 kg/m^3 due to the

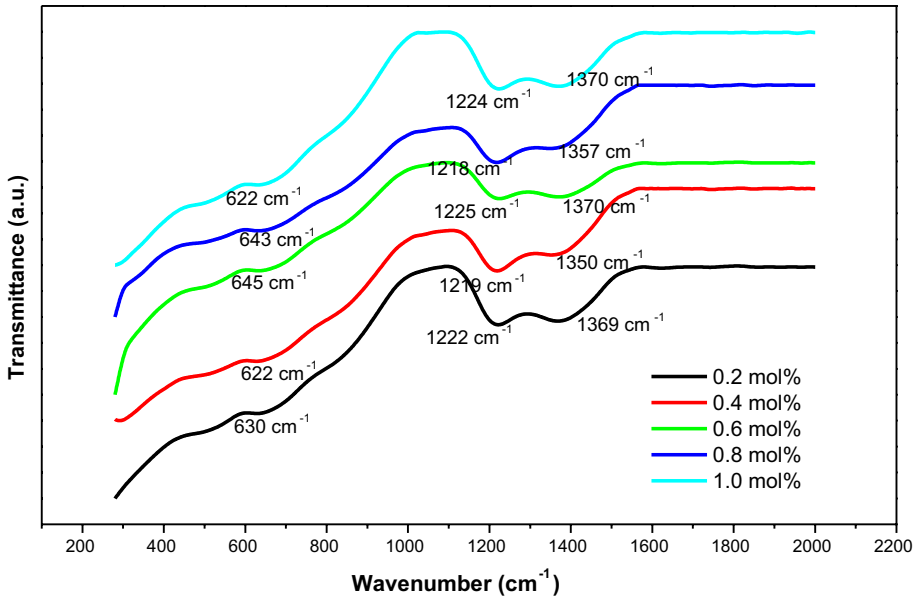

Fig. 3 FTIR transmittance spectra of $(1-x)[(TeO_2)_{70}(B_2O_3)_{30}]$-$x(Gd_2O_3)$ glasses

Table 3 Density, molar volume and refractive index of $(1-x)$ $[(TeO_2)_{70}$ $(B_2O_3)_{30}]$-$x(Gd_2O_3)$ glasses

Mol%, x (Gd_2O_3)	Density (kg/m^3)	Molar volume (m^3/mol)	Experimental refractive index, n (632.80 nm) ± 0.01	Theoretical refractive index, n
0.2	3914	3.40×10^{-5}	2.029	2.535
0.4	4045	3.30×10^{-5}	1.940	2.529
0.6	3959	3.38×10^{-5}	1.951	2.543
0.8	4014	3.35×10^{-5}	1.964	2.538

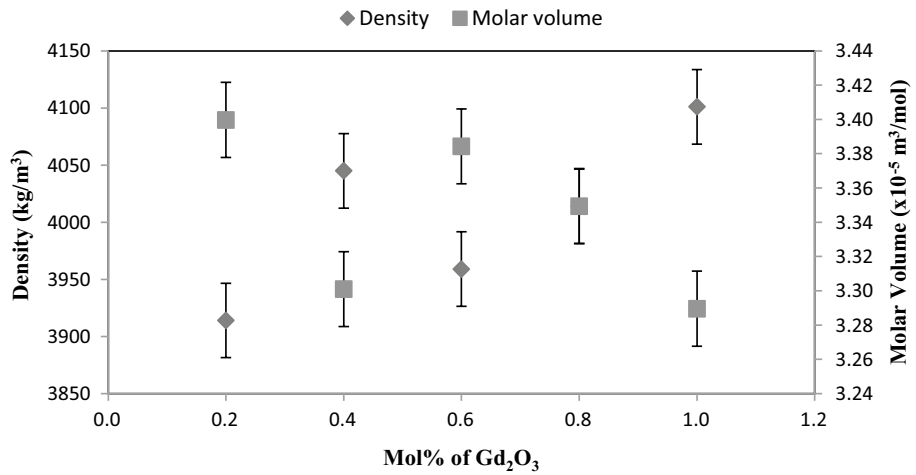

Fig. 4 Density and molar volume of $(1-x)$ $[(TeO_2)_{70}(B_2O_3)_{30}]$-$x(Gd_2O_3)$ glasses

increase of Gd_2O_3 mol% can be attributed to the substitution of lower molecular weight substance, TeO_2 (atomic mass, Z_{TeO_2} = 159.5988 gmol^{-1}) and B_2O_3 (atomic mass, $Z_{B_2O_3}$ = 69.6202 gmol^{-1}), by higher molecular weight substance, Gd_2O_3 (atomic mass, $Z_{Gd_2O_3}$ = 362.4982 gmol^{-1}), leading to an increase in the net molecular weight of the glass systems [16]. The increasing number of oxygen atoms and Gd cations radius due to higher atomic weight of Gd atoms contributes to higher packing density [16]. Conversely, the molar volume of the present glass samples is found to decrease from 3.40×10^{-5} to 3.29×10^{-5} m^3/mol as shown in Fig. 4. This can be ascribed to the inverse relation between density and molar volume [16]. Hence, the increase in density will lead to decrease molar

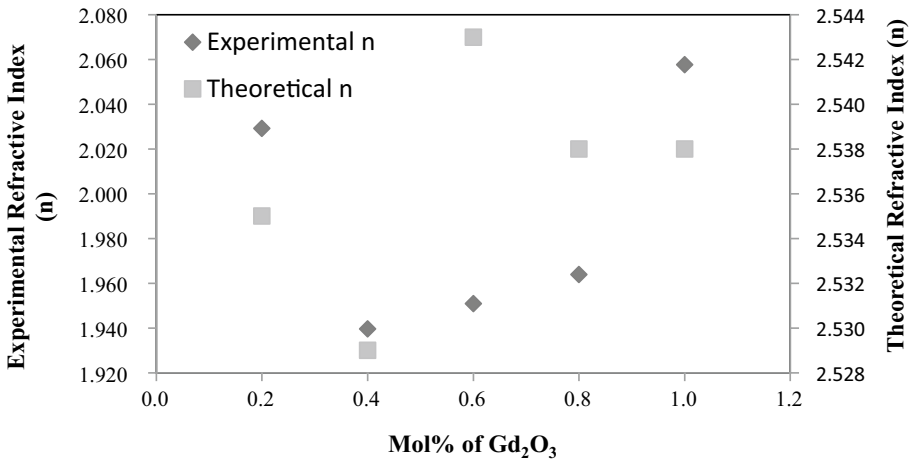

Fig. 5 Refractive index for $(1-x)[(TeO_2)_{70}(B_2O_3)_{30}]$-$x(Gd_2O_3)$ glasses

volume. The presence of Gd_2O_3 in the glass matrix leads to change in bond length or inter-atomic spacing between the atoms, and the rearrangement of lattice within the vitreous network also contributed to the variation in molar volume [22].

Refractive index

The values of experimental refractive index, *n* (632.80 nm), are recorded in Table 3 and are presented in Fig. 5 for different compositions of Gd_2O_3. It is observed that the refractive index of the gadolinium oxide-doped tellurite glasses decreases from 2.029 to 1.940 with initial addition of Gd_2O_3 to the glass system. However, with further inclusion of Gd_2O_3 to the glass matrix, the refractive index of the glasses increases from 1.940 to 2.058. The decrement in refractive index is interconnected to the structural change from TeO_3 to TeO_4 and formation of bridging oxygen atoms after addition of Gd ions into the glass formation. This is because bridging oxygen atoms have lower polarizability as compared to non-bridging oxygen atoms [16, 17]. Nevertheless, with further increment of Gd_2O_3 in the glass network, the effect of large ions Gd ions became more pronounce. This is because Gd^{3+} ions (1.79 Å) which are higher than the atomic radius of tellurite atom (1.6 Å) and boron atom (0.98 Å) into the network improve the refractive index. These are due to high cation polarization possessed by Gd ions corresponding from enlargement of cation size. The higher values of refractive index observed have potential application in nonlinear optical materials.

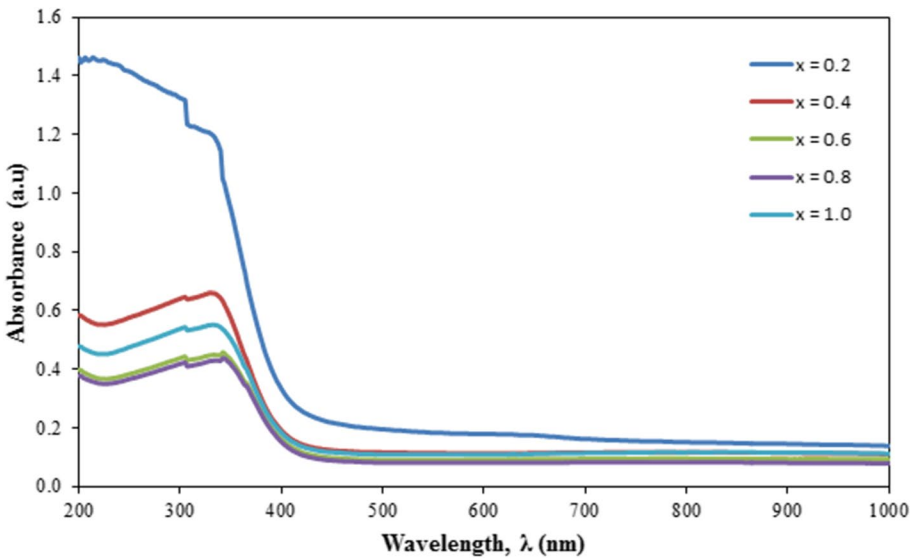

Fig. 6 Optical ABSORBANCE spectra for $(1-x)[(TeO_2)_{70}(B_2O_3)_{30}]$-$x(Gd_2O_3)$ glasses

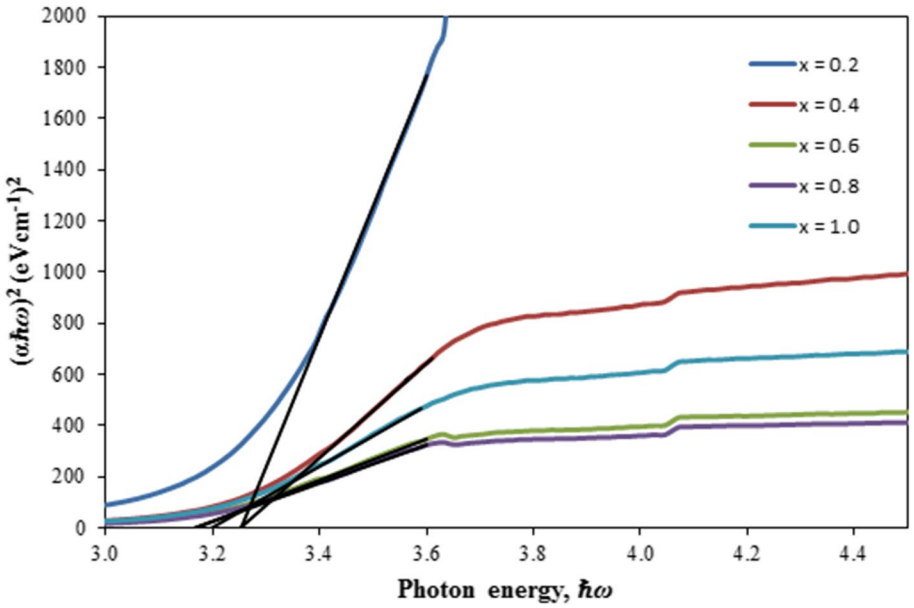

Fig. 7 Direct energy band gap of $(1-x)[(TeO_2)_{70}(B_2O_3)_{30}]$-$x(Gd_2O_3)$ glasses

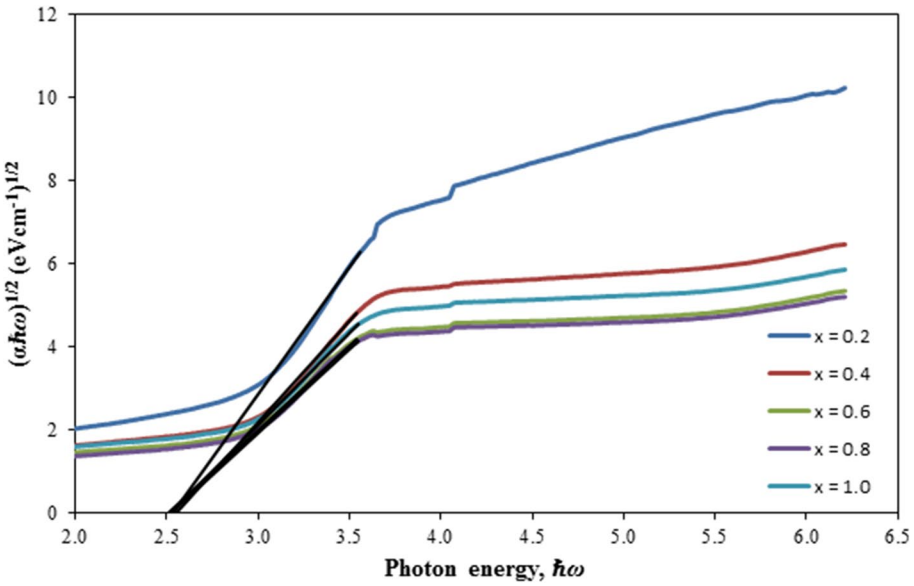

Fig. 8 Indirect energy band gap of $(1-x)[(TeO_2)_{70}(B_2O_3)_{30}]$-$x(Gd_2O_3)$ glasses

Optical absorption and optical band gap

Figure 6 presents the absorption spectra of gadolinium oxide-doped tellurite glasses and the absorption coefficient, $\alpha(\omega)$, near the absorption edge and will be calculated by the following formula:

$$\alpha(\omega) = 2.303\frac{A}{d} \tag{1}$$

where A is the absorbance and d corresponds to the thickness of the glass samples [16–19, 23]. The optical absorption edge does not exhibit any sharp absorption edges which are in agreement with the XRD spectra as shown in Fig. 1 indicating the samples produced are non-crystalline material. The relationship between optical band gap energy, E_{opt}, and the absorption coefficient, $\alpha(\omega)$, is given by Eq. (2):

$$\alpha(\omega) = \frac{B\left(\hbar\omega - E_{opt}\right)^n}{\hbar\omega} \tag{2}$$

where B is constant, E_{opt} is the energy of optical band gap, $\hbar\omega$ is the photon energy and $\alpha(\omega)$ is the absorption coefficient as reported in. The values of n are $1/2$ and 2 for the allowed direct and allowed indirect transitions, respectively. Both direct and indirect band gaps obtained from Eq. (2)

Table 4 Direct energy band gap E^1_{opt}, indirect energy band gap E^2_{opt} and Urbach energy (ΔE) of $(1-x)[(TeO_2)_{70}(B_2O_3)_{30}]$-$x(Gd_2O_3)$ glasses

Mol%, x (Gd_2O_3)	Direct energy band gap, E^1_{opt} (eV)	Indirect energy band gap, E^2_{opt} (eV)	Urbach energy, ΔE (eV)
0.2	3.253	2.535	0.397
0.4	3.252	2.555	0.359
0.6	3.168	2.511	0.353
0.8	3.167	2.526	0.351

depend on the inter-band transitions, but latter involves the phonon interactions [16]. The relationship between $(\alpha\hbar\omega)^2$ and photon energy ($\hbar\omega$) and $(\alpha\hbar\omega)^{1/2}$ against ($\hbar\omega$) is plotted (Figs. 7 and 8) to determine the ability the best fitting into direct and indirect optical band gap formula for the optical data on the glass. The value of optical band gap (E_{opt}) for either direct or indirect can be acquired by extrapolating the linear parts of the curves and tabulated in Table 4.

It is observed that the direct and indirect energy band gap decreased from 3.253 to 3.199 and from 2.535 to 2.525 eV with increasing Gd_2O_3. The disarray in the glass structure leads to further extension of the localized states into the gap according to Mott and Davies as used before [16]. The decrement observed can be attributed to the partial conversion of BO_4 to BO_3 structural units with the formation of non-bridging oxygen atoms. This is because the electrons are less tightly bound to the nuclear charge and easily excite from the valence to conduction band. Moreover, the presence of trivalent Gd ions affects the network structure of the glass sample by increasing the number of free electrons leading to decrease band gap energy. The high field strength possessed by Gd ions which can be polarized easily also contributed to the decrement in optical band gap. The values of the band gap energy obtained have potential photonic applications. Absorption edge usually follows Urbach rule as follows:

$$\alpha(\omega) = \alpha_0 \exp(\hbar\omega/\Delta E) \tag{3}$$

where α_0 is a constant and ΔE is a measure of the band tailing and is known as Urbach energy as reported in [16]. Values of ΔE decreased from 0.397 to 0.354 as shown in Table 4 and Fig. 9. The values of Urbach energy ΔE decrease with increasing Gd_2O_3 content which causes the fragility nature of the vitreous network to decrease. The changes in Urbach energy are due to the change in the structural units within the vitreous after the inclusion of Gd_2O_3. The Urbach energy obtained is in the range of amorphous semiconductor 0.046 to 0.66 eV.

Thermal diffusivity

The thermal diffusivity β is the rapidity of the heat propagating through the material [20, 21, 24–26] which has been calculated according to Eq. 4.

$$\beta = \frac{0.1388L^2}{t_{1/2}} \tag{4}$$

where L is the thickness of the glass material and $t_{1/2}$ is the time required for the back specimen to reach half the maximum temperature rise as reported in. The variation of the thermal diffusivity of gadolinium oxide-doped tellurite glasses varies from 2.32172×10^{-7} to 2.09430×10^{-7} to 2.46902×10^{-7} m^2/s as the concentration of Gd_2O_3 increases from 0.2 to 1.0 mol% as shown in Fig. 10 and Table 5. Thermal diffusivity of gadolinium

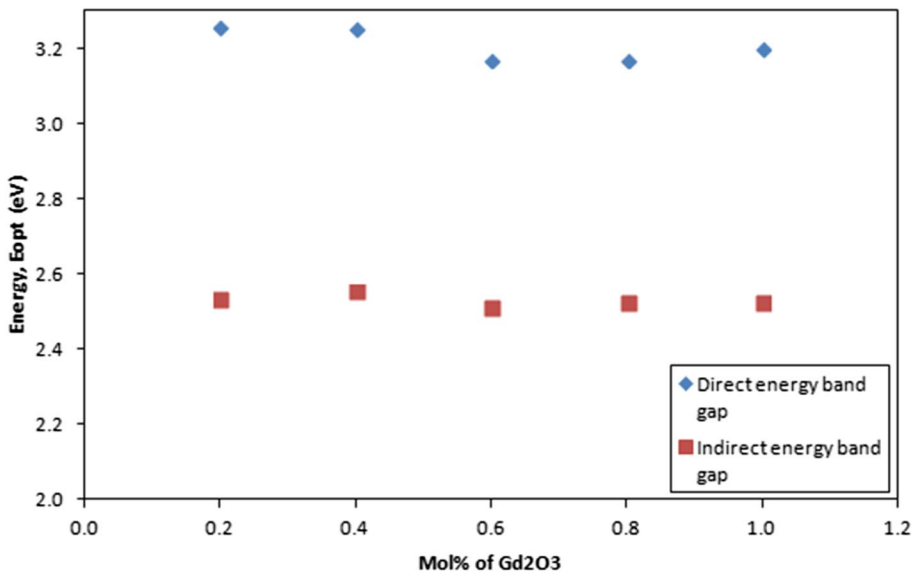

Fig. 9 Variation of direct and indirect optical band gap for $(1-x)[(TeO_2)_{70}(B_2O_3)_{30}]$-$x(Gd_2O_3)$ glasses

oxide-doped tellurite glass peaked itself at $x = 1.0$ mol% with value 2.46902×10^{-7} m^2/s, which is lower than that of window glass 3.4×10^{-7} m^2/s. Also, the present values are lower as compared with the results obtained by other tellurite glasses, 2.7 to 3.0×10^{-7} m^2/s and from 3.1 to 3.4×10^{-7} m^2/s as reported in. In previous research [20, 21, 24–26], it has been reported that a maximum in thermal diffusivity has a minimum molar volume. Moreover, on adding B_2O_3 into TeO_2 network, the optical and dielectric properties constant remains practically the same, but the thermal stability

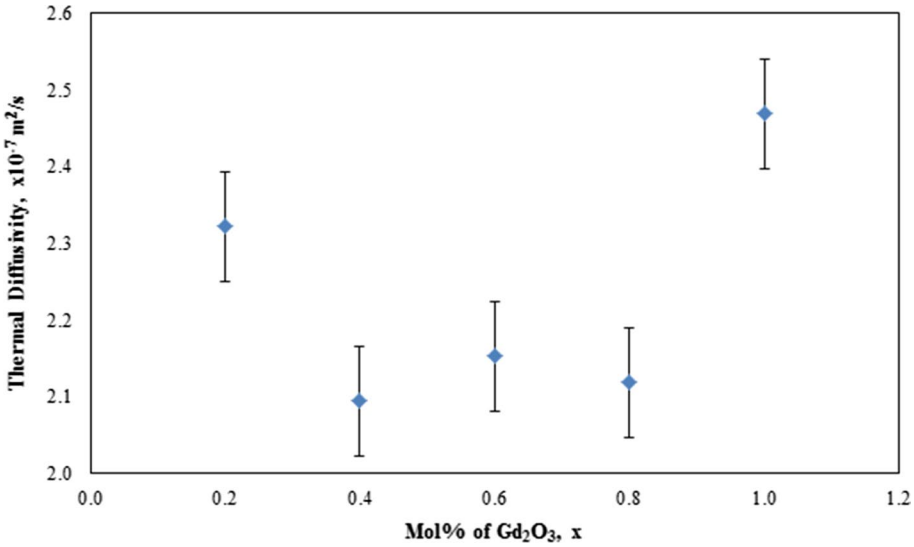

Fig. 10 Thermal diffusivity of $(1-x)[(TeO_2)_{70}(B_2O_3)_{30}]$-$x(Gd_2O_3)$ glasses

Table 5 Thermal diffusivity of $(1-x)[(TeO_2)_{70}(B_2O_3)_{30}]$-$x(Gd_2O_3)$ glasses

Mol%, x (Gd_2O_3)	Thickness L (m)	Time t (s)	Thermal diffusivity β ($\times 10^{-7}$ m^2/s)	Error ($\times 10^{-9}$ m^2/s)
0.2	0.00249	4.062	2.32172	4.64344
0.4	0.00249	4.464	2.09430	4.18860
0.6	0.00247	4.308	2.15262	4.30525
0.8	0.00250	4.453	2.11854	4.23708
1.0	0.00250	3.872	2.46902	4.93803

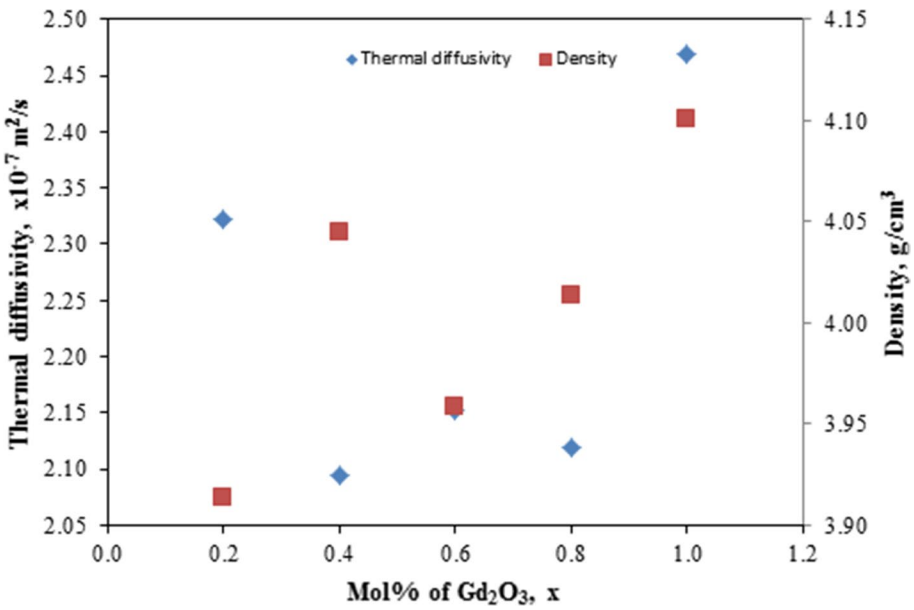

Fig. 11 Thermal diffusivity and density of $(1-x)[(TeO_2)_{70}(B_2O_3)_{30}]$-$x(Gd_2O_3)$ glasses

contrary to devitrification intensifies considerably [1]. The changes in the thermal diffusivity can be attributed to the size of the rare-earth ion, Gd ions. When TeO_2–B_2O_3 is substituted by the bigger atom Gd_2O_3, there is expansion in the size of the atom within the glass network which causes the mean free path to increase, and hence, there is an increase in thermal diffusivity. Therefore, at $x = 1.0$ mol%, the content of the gadolinium atom is the highest and it gives the highest value of the thermal diffusivity which is desirable for photonic application because it can be used to avoid thermal loading during the excitation processes. In Fig. 11, it is noted that when density increases, thermal diffusivity decreases and vice versa. This behaviour may be explained by the substitution of gadolinium atom, Gd_2O_3, in the glass network. As explained in the previous part, gadolinium atom has higher atomic weight (362.5 g/mol) than borotellurite atoms (229.2 g/mol). Therefore, the change of thermal diffusivity is due to the change in density. Also, Fig. 12 shows that at the point with highest thermal diffusivity value, it has the smallest molar volume. The glass system with minimum molar volume may due to the closely packing of the structure network. Decreasing in molar volume may cause the inter-atomic distance to decrease and compactness of glass network to increase. Therefore, with a short distance for the vibration of molecules in the lattice or phonon, the heat energy can be transported faster. The high thermal diffusivity will lead to high thermal conductivity because there is a direct relationship between thermal diffusivity and thermal conductivity. Hence, the high thermal diffusivity is useful in the design of high-power nonlinear optical devices. This is because materials with high thermal diffusivity allow rapid extraction of the heat produced by the absorption of optical energy to avoid the reduction in efficiency and beam quality as well as to enhance the average power outputs of the dev ices.

Electronic polarizability, optical basicity and metallization criterion

Electronic polarizability is crucial to determine the suitability of the studied materials as optoelectronic devices because they are highly related to conductivity, third-order optical nonlinearity and linear optical properties. The value of electronic polarizability can be estimated by using mathematical approach proposed by Clausios–Mossotti where the equation is given by [27]

$$\alpha_m = \frac{3}{4\pi N_A} R_m \tag{5}$$

where N_A is the Avogadro's number.

The chemical interaction between the components of the oxide glasses consists of acid-based character. Based on the Lewis theory, a base comprises at least one pair of valence electron that is not being shared by other molecules. Meanwhile, an acid consists of a vacant orbital that can be accommodated by other ions. It is of interest to study the ability of the oxygen to transfer the negative charge into weak cations surrounding. The value of optical basicity Λ was calculated by using relation as follows [22].

$$\Lambda = X_1\Lambda_1\Lambda = \quad \Lambda = X_1\Lambda_1 + X_2\Lambda_2 + \cdots + X_n\Lambda_n \tag{6}$$

where $X_1, X_2, \ldots, X_n$ correspond to the equivalent fractions of oxides and $\Lambda_1, \Lambda_2, \ldots, \Lambda_n$ correspond to the optical basicity of oxides in the studied glass system. The condition of $R_m/V_m = 1$ in the Lorentz–Lorenz equation described that the refractive index becomes infinite. This is in accordance

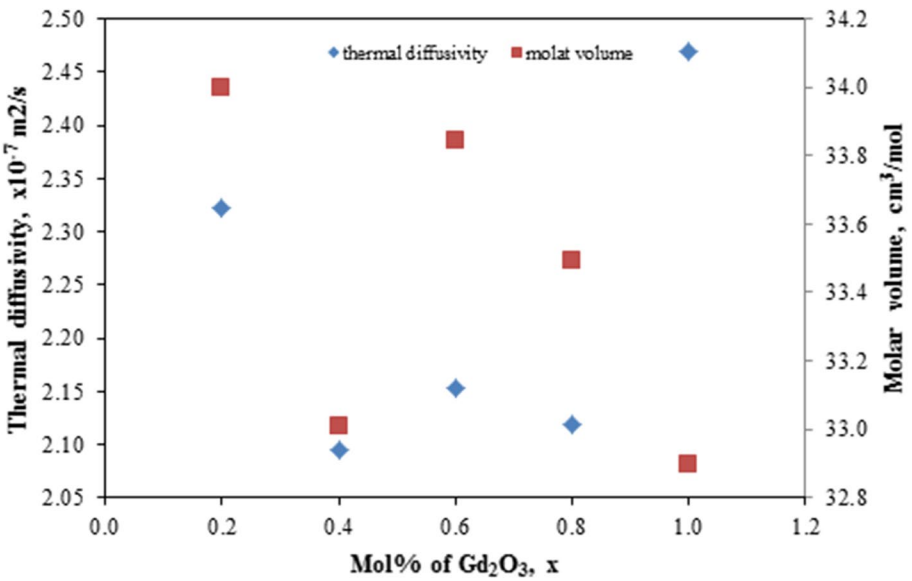

Fig. 12 Thermal diffusivity and molar volume of $(1-x)[(TeO_2)_{70}(B_2O_3)_{30}]$-$x(Gd_2O_3)$ glasses

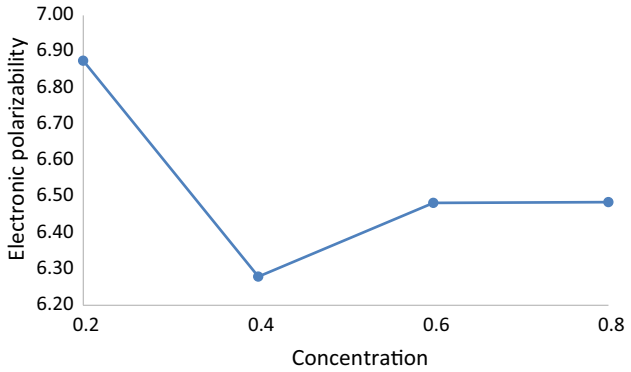

Fig. 13 Electronic polarzability of $(1-x)[(TeO_2)_{70}(B_2O_3)_{30}]$-$x(Gd_2O_3)$ glasses

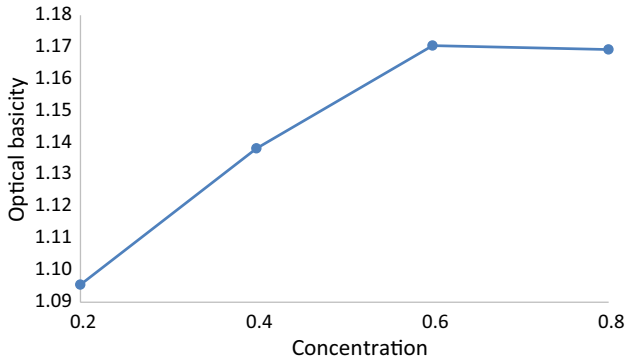

Fig. 14 Optical basicity of $(1-x)[(TeO_2)_{70}(B_2O_3)_{30}]$-$x(Gd_2O_3)$ glasses

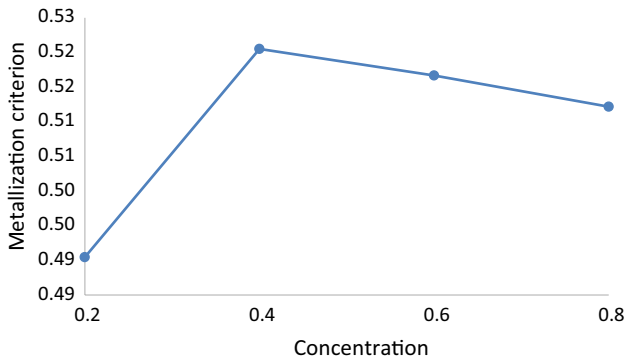

Fig. 15 Metallization criterion of $(1-x)[(TeO_2)_{70}(B_2O_3)_{30}]$-$x(Gd_2O_3)$ glasses

with the metallization of covalent solid materials. In other words, the electrons become itinerant and acquires metallic status. The nature of metallic and non-metallic of oxide glasses can be predicted by the following conditions: $R_m/V_m < 1$ (non-metal) and $R_m/V_m > 1$ (metal). It is important to determine the tendency of the glass sample towards metallic/non-metallic properties. The value of metallization criterion was obtained by using an equation as follows [22].

$$M = 1 - \frac{R_m}{V_m} \tag{7}$$

where R_m is the molar refraction and V_m is the molar volume. The trend of electronic polarizability, optical basicity and metallization criterion along with gadolinium oxide is shown in Figs. 13, 14 and 15. Electronic polarzabilty, optical basicity and metallization criterion were 6.5 to 6.28 (Å), 1.095 to 1.17 and 0.49 to 0.52, respectively. It can be seen from the figure that the trend of electronic polarizability is found with the highest value at 0.2 mol fraction and minimum at 0.4 mol fraction. The maximum value of electronic polarizability reflects the value of refractive index which is high at 0.2 mol fraction. The formation of glass network is based on the conversion of bridging oxygen to non-bridging oxygen. It is known that the lone pair of electrons in the bridging oxygen has high mobility which results in high tendency to polarize. The low number of electronic polarizability at 0.4 mol fraction represents the low ability of electrons to polarize. The reduction in the number of non-bridging oxygen may contribute to the decrease in polarizing power in the glass system. However, the electronic polarizability starts to increase at 0.6 and 0.8 mol fraction. The overall values of electronic polarizability are relatively large, and it is suggested that the glass system has high potential in linear and nonlinear optical materials.

Conclusion

The $(1-x)[(TeO_2)_{70}(B_2O_3)_{30}]$-$x(Gd_2O_3)$ with $x = 0.2$, 0.4, 0.6, 0.8 and 1.0 mol% glasses have been prepared successively, and the effect of replacing TeO_2 by (Gd_2O_3) is as follows:

1. Density increases with gadolinium oxide due to the replacement of lower molecular weight element with larger molecular weight element. The molar volume of the amorphous materials decreases as Gd_2O_3 increases.
2. FTIR results shows three vibrational bands around 621–646 cm^{-1}, 1217–1225 cm^{-1} and 1349–1371 cm^{-1} which are ascribed to TeO_4 and BO_3 structural units. Besides that, the presence of large Gd cations causes the change in refractive index observed.
3. Direct and indirect optical band gap energy decreases with Gd_2O_3 due to the formation of non-bridging oxygen resulting from partial conversion of BO_4 to BO_3 structural units.

4. In addition, the decreasing trend shown in Urbach energy suggests that the fragility of the glass network decreases.
5. Thermal diffusivity of glass samples was investigated, and it is found that thermal diffusivity of gadolinium oxide-doped tellurite glass peaked itself at 1.0 mol% with value 2.46902×10^{-7} m^2/s and is also related to the substitution by bigger atom.
6. Electronic polarzabilty, optical basicity and metallization criterion were 6.5 to 6.28 (Å), 1.095 to 1.17 and 0.49 to 0.52, respectively.

Acknowledgements This research was financially supported by Geran Penyelidikan Universiti (GPU), Sultan Idris Education University (Grant Code: 2018-0139-103-01) and Skim Geran Penyelidikan Fundamental (FRGS) Fasa 1/2018 (Grant Code: 2019-0006-102-02). The authors would like to thank the following institutions for equipment support: Faculty of Science and Mathematics, Universiti Pendidikan Sultan Idris and Faculty of Science, Universiti Putra Malaysia.

References

1. Maheshvaran, M., Linganna, K., Marimuthu, K.: Composition dependent structural and optical properties of Sm^{3+} doped borotellurite glasses. J. Lumin. **131**, 2746–2753 (2011)
2. Selvaraju, K., Marimuthu, K.: Structural and spectroscopic studies on Er^3 doped boro-tellurite glasses. Phys. B **40**, 1086–1093 (2012)
3. Azlan, M., Halimah, M., Shafinas, Z.S., Daud, W.: Effect of erbium nanoparticles on optical properties of zinc borotellurite glass system. J. Nanomater. **2013**, 8 (2013)
4. El-Mallawany, R.: Preface, tellurite glasses—structure, properties and applications. J. Non-Cryst. Solids **533**, 119905 (2020)
5. Ali, A.A., Rammah, Y.S., El-Mallawany, R., Souri, D.: FTIR and UV spectra of pentaternary borate glasses. J. Meas. **105**, 72 (2017)
6. Sahar, M., Sazali, E.: Physical and thermal properties of TeO_2-Na_2O-MgO doped Eu_2O_3 glass. Empower. Sci. Technol. Innov. Towards Better Tomorrow **PCO10**, 62–68 (2011)
7. El-Mallawany, R.: Structural interpretations on tellurite glasses. Mater. Chem. Phys. **63**, 109 (2000)
8. Oo, M., Halimah, M., Daud, W.: Optical properties of bismuth tellurite based glass. Int. J. Mol. Sci. **13**, 4623–4631 (2012)
9. El-Mallawany, R.: Quantitative analysis of elastic moduli of tellurite glasses. J. Mater. Res. **5**, 2218 (1990)
10. Kundu, R., Dhankhar, S., Punia, R., Sharma, S., Kishore, N.: $ZnCl_2$ modified physical and optical properties of barium tellurite glasses. Trans. Indian Ceram. Soc. **72**, 206–210 (2013)
11. Mahraz, Z.S., Sahar, M., Ghoshal, S.: Band gap and polarizability of boro-tellurite glass: influence of erbium ions. J. Mol. Struct. **1072**, 238–241 (2014)
12. El-Adawi, A., El-Mallawany, R.: Elastic modulus of tellurite glasses. J. Mater. Sci. Lett. **15**, 2065 (1996)
13. Joshi, C., Dwivedi, Y., Rai, S.: Structural and optical properties of Ho_2TeO_6 micro-crystals embedded in tellurite matrix. Ceram. Int. **37**, 2603–2608 (2011)
14. Chen, Y., Nie, Q., Xu, T., Dai, S., Wang, X., Shen, X.: A study of nonlinear optical properties in Bi_2O_3-WO_3-TeO_2 glasses. J. Non-Cryst. Solids **354**, 3468–3472 (2008)
15. Fudzi, F., Kamari, H., Abd, A., Noorazlan, A.: Linear optical properties of zinc borotellurite glass doped with lanthanum oxide nanoparticles for optoelectronic and photonic application. J. Nanomater **4150802**, 8 (2017)
16. Elkhoshkhany, N., Abbas, R., El-Mallawany, R., Fraih, A.: Optical properties of quaternary TeO_2–ZnO–Nb_2O_5–Gd_2O_3 glasses. Ceram. Int. **40**, 14477–14481 (2014)
17. Singh, L., Thakur, V., Punia, R., Kundu, R., Singh, A.: Structural and optical properties of barium titanate modified bismuth borate glasses. Solid State Sci. **37**, 64–71 (2014)
18. Rao, S.L.S., Ramadevudu, G.S., Hameed, M.Md.A., Chary, N., Rao, M.L.: Optical properties of alkaline earth borate glasses. Int. J. Eng. Sci. Technol. **4**, 25–35 (2012)
19. Kundu, R., Dhankhar, S., Punia, R., Nanda, K., Kishore, N.: Bismuth modified physical, structural and optical properties of mid-IR transparent zinc boro-tellurite glasses. J. Alloy. Compd. **587**, 66–73 (2014)
20. Ridha, N., Yunus, W., Halim, S., Talib, Z., Al-Asfoor, F., Primus, W.: Effect of Sr substitution on structure and thermal diffusivity of Ba1-xSrxTiO$_3$ ceramic. Am. J. Eng. Appl. Sci. **2**, 661–664 (2009)
21. Lima, S., Falco, W., Bannwart, E., Andrade, L., Oliveira, R., Moraes, J., Baesso, M.: Thermo-optical characterization of tellurite glasses by thermal lens, thermal relaxation calorimetry and interferometric methods. J. Non-Cryst. Solids **352**, 3603–3607 (2006)
22. Dimittrov, V., Komatsu, T.: An interpretation of optical properties of oxides and oxides glasses in term of electronic polarizability and average single bond strength. J. Univ. Chem. Technol. Metall. **45**, 219–250 (2010)
23. Mhareb, M., Hashim, S., Ghoshal, S., Alajerami, Y., Saleh, M., Dawaud, R., Azizan, S.: Impact of Nd^{3+}ions on physical and optical properties of lithium magnesium borate glass. Opt. Mater. **37**, 391–397 (2014)
24. Moraes, J., Nardi, J., Sidel, S., Mantovani, B., Yukimitu, K., Reynoso, V., Lima, M.: Relation among optical, thermal and thermo-optical properties and niobium concentration in tellurite glasses. J. Non-Cryst. Solids **356**, 2146–2150 (2010)
25. Sampaio, J., Gama, S., Baesso, S., Catunda, T.: Fluorescence quantum efficiency of Er^{3+} in low silica calcium aluminate glasses determined by mode-mismatched thermal lens spectroscopy. J. Non-Cryst. Solids **351**, 1594–1602 (2005)
26. Beasley, J.: Thermal conductivities of some novel nonlinear optical materials. Appl. Opt. **33**, 1000 (1994)
27. Hampton, R.N., Hong, W., Saunders, G.A., El-Mallawany, R.: Dielectric properties of tellurite glasses. Phys. Chem. Glasses **29**, 100–105 (1988)